Journal of Statistical Physics, Vol. 75, Nos. 3/4, 1994

Pattern Formation by Growing Droplets: The Touch-and-Stop Model of Growth

Yu. A. Andrienko,[1] N. V. Brilliantov,[1,2] and P. L. Krapivsky[3]

Received September 2, 1993; final January 3, 1994

We investigate a novel model of pattern formation phenomena. In this model spherical droplets are nucleated on a substrate and grow at constant velocity; when two droplets touch each other they stop their growth. We examine the heterogeneous process in which the droplet formation is initiated on randomly distributed centers of nucleation and the homogeneous process in which droplets are nucleated spontaneously at constant rate. For the former process, we find that in arbitrary dimension d the system reaches a jamming state where further growth becomes impossible. For the latter process, we observe the appearance of fractal structures. We develop mean-field theories that predict that the fraction of uncovered material $\Phi(t)$ approaches to the jamming limit as $\Phi(t)-\Phi(\infty)\sim\exp(Ct^d)$ for the heterogeneous process and as a power law for the homogeneous process. Exact solutions in one dimension are obtained and numerical simulations for $d=1$–3 are performed and compared with mean-field predictions.

KEY WORDS: Pattern formation; nucleation and growth; fractals.

1. INTRODUCTION

Numerous examples of spatial pattern formation processes may be found in metallurgical, polymeric, ceramic, crystalline, chemical, and biological systems.[1–3] The formation of dew on leaves and cobwebs; breath figures on nonwetting substrates[4]; soap bubbles[5]; microemulsion[6]; fog, rain, and clouds[7]; glasses and amorphous materials[8]; porous media[9]; thin films[10]; and territories among competing animals[11] are some of the

[1] Department of Physics, Moscow State University, Moscow 119899, Russia.
[2] Max-Planck AG "Nichtlineare Dynamik," Potsdam University, D-14415, Potsdam, Germany.
[3] Center for Polymer Studies and Department of Physics, Boston University, Boston, Massachusetts 02215.

0022-4715/94/0500-0507$07.00/0

possible examples. Understanding the kinetics of their formation is a challenging problem of considerable practical and theoretical interest.

A number of pattern formation phenomena may be described by a random sequential adsorption (RSA) model.[12] In this model particles are placed randomly and sequentially onto a substrate and they cannot adsorb on top of previously adsorbed ones. RSA processes usually continue until a jamming configuration, where further adsorption events are impossible. A notable feature of the RSA processes is that the pattern is formed by particles of prescribed shape and size which do not change during the process.

Another important class of pattern formation processes is related to nucleation and growth phenomena. A toy model of such processes is the Kolmogorov or Johnson–Mehl–Avrami model of phase transformation kinetics.[13] In this model, small spherical seeds are nucleated at a constant rate per unit volume in the metastable phase and grow at constant velocity once formed (homogeneous nucleation) or seeds are nucleated in the metastable phase on defects (heterogeneous nucleation). Contrary to the RSA model, both the size and the shape of droplets change during the evolution in this model.

In this article, we investigate a pattern formation model intermediate between the RSA model and the Kolmogorov–Johnson–Mehl–Avrami model. We assume that the pattern is formed by growing droplets of prescribed spherical shape. The condition of shape persistence modifies the rule of growth: when two (or more) droplets touch they stop their growth and remain permanently fixed. This model will be called the touch-and-stop model.

In general, the process of droplet formation proceeds either by spontaneous nucleation or by growth from the centers of nucleation. We consider two models describing these two types of nucleation. In the homogeneous nucleation model, vanishingly small spherical droplets are nucleated at a constant rate I per unit volume in the metastable phase and then grow at constant velocity V. The heterogeneous nucleation model is obtained by placing randomly at time $t=0$ nuclei with density γ which initiate then the phase transformation process.

A variety of application of the model may be envisioned. The shape persistence of the growing droplets may be caused by a number of reasons. For example, it may be a strong surface tension that prevents the droplets from having any shape different from the spherical one; on the other hand, a strong interaction with a substrate may prevent droplets from coalescing. Note also that the homogeneous variant of the present touch-and-stop model is a generalized dynamic version of the random space-filling-bearing model[14,15] which is in fact a random version of Apollonian packing.[16]

It has been speculated that the random space-filling-bearing model may mimic a variety of natural phenomena ranging from the motion of matter in seismic gaps up to some aspects of turbulence.[14] However, the growth velocity in the random space-filling-bearing model is considered as infinitely large. Hence after a nucleation event a droplet touches the closest stationary droplet and stops its growth immediately. Moreover, the model is nontrivial only if a typical size of the system is finite (e.g., if the process takes place in a hole between three touching discs as in the Apollonian packing[16] or in a strip). On the other hand, our model is well defined for infinite systems and probably may mimic the kinetics of a number of natural phenomena.

The rest of this paper is organized as follows. In Section 2, we develop a mean-field theory (MFT) for both homogeneous and heterogeneous nucleation processes in d dimensions. Both models are solved exactly in Section 3. In Section 4, we present the results of numerical simulations, compare numerical and exact results in one dimension, and describe the geometric structure of final patterns. Finally, we summarize our findings in Section 5.

2. MEAN-FIELD APPROACH

We start by developing a mean-field approximation for a simpler heterogeneous variant of the touch-and-stop model. Denote by $N(t) = 1 - \Phi(t)$ the fraction of material that has not been transformed before time t. If we ignore the overlap of growing spheres, we readily obtain $N(t) = \gamma\Omega_d (Vt)^d$, where $\Omega_d = \pi^{d/2}/\Gamma(1 + d/2)$ is the volume of a d-dimensional unit sphere. This is of course an overestimate of $N(t)$. First we derive the upper and lower estimates for $\Phi(t)$ by taking into account the reduction of $N(t)$ due to the nearest-neighbor interaction. Since the nucleation centers are distributed randomly, the nearest-neighbor distance is given by the Hertz form (see, e.g., ref. 17)

$$p(r) = d\gamma\Omega_d r^{d-1} e^{-\gamma\Omega_d r^d} \tag{1}$$

So, we find

$$\frac{dN}{dt} = d\gamma\Omega_d V^d t^{d-1} \int_{2Vt}^{\infty} d\gamma\Omega_d r^{d-1} e^{-\gamma\Omega_d r^d}\, dr \tag{2}$$

Solving Eq. (2) yields

$$\Phi_{\text{upper}}(t) = 1 - 2^{-d} + 2^{-d} e^{-\gamma\Omega_d (2Vt)^d} \tag{3}$$

Note that Eq. (3) provides the upper bound for the actual fraction of

untransformed material because the nearest-neighbor droplet that was implicitly assumed growing all the time before touching with the examined one could already be stopped by touching with other droplets. Technically, this assumption was made in writing the lower limit of the integral in the right-hand side of Eq. (2).

To derive a lower bound $\Phi_{\text{lower}}(t)$, one should replace the lower limit in the integral in the right-hand side of Eq. (2) by Vt. This accounts for the opposite extreme situation when the nearest-neighbor droplet stops immediately at $t=0$:

$$\frac{dN}{dt} = d\gamma\Omega_d V^d t^{d-1} \int_{Vt}^{\infty} d\gamma\Omega_d r^{d-1} e^{-\gamma\Omega_d r^d}\, dr \tag{4}$$

From (4) one gets

$$\Phi_{\text{lower}}(t) = e^{-\gamma\Omega_d (Vt)^d} \tag{5}$$

Observe that the lower bound coincides with the well-known exact result obtained for the Kolmogorov–Johnson–Mehl–Avrami nucleation and growth model.[13] While the lower bound (5) fails to predict a nontrivial jammed state, $\Phi_{\text{lower}}(\infty)=0$, the rate of relaxation appears to be true. This follows from the well-known Lifshitz argument[18] since the long-time behavior is governed by a large empty region transforming by long-living droplets nucleated near centers of these regions. On the other hand, the upper bound (3) predicts a nontrivial jammed state, $\Phi_{\text{upper}}(\infty)=1-2^{-d}$, but the approach to the jammed state is too rapid.

Let us turn now from the upper and lower bounds to the mean-field approximation for the touch-and-stop model with heterogeneous nucleation. We develop the MFT by more accurate accounting for the touch-and-stop process compared to those used previously in deriving Eqs. (3) and (5). To this end we introduce the function $\Psi(t)$, the probability that the growth of a droplet has not been stopped before time t. In a mean-field spirit, one can estimate $\Psi(t)$ as the product of $\exp[-\gamma\Omega_d (Vt)^d]$, the probability that the distance from a droplet to the nearest one is greater than Vt, and

$$[1 - d\gamma\Omega_d V^d (t+t')^{d-1}\, \Psi(t')\, dt'] = \exp[-d\gamma\Omega_d V^d (t+t')^{d-1}\, \Psi(t')\, dt']$$

the probabilities that a droplet has not been stopped by droplets nucleated in a region between spheres of radii $V(t+t')$ and $V(t+t'+dt')$. Multiplying these factors, we find

$$\Psi(t) = \exp\left[-\gamma\Omega_d (Vt)^d - d\gamma\Omega_d V^d \int_0^t (t+t')^{d-1}\, \Psi(t')\, dt' \right] \tag{6}$$

The fraction of the material which has been transformed before time t is

$$N(t) = d\gamma\Omega_d V^d \int_0^t (t')^{d-1}\, \Psi(t')\, dt' \tag{7}$$

It is worth pointing out that if we assume $\Psi(t) = 1$ as the first approximation and then substitute this value into the right-hand side of Eq. (6), we arrive at the more accurate result for $\Psi(t)$, $\Psi(t) = \exp[-\gamma\Omega_d (2Vt)^d]$. By inserting this result into Eq. (7), one can rederive the upper bound (3). Similarly, by assuming $\Psi(t) = 0$ as the first approximation, one can rederive the lower bound (5).

We cannot solve nonlinear integral equation (6) analytically in arbitrary dimension. However, in one dimension we have succeeded in finding the exact solution of this equation, which reads

$$\Phi(t) = 1 - \log(2 - e^{-2\gamma Vt}) \tag{8}$$

Nevertheless for arbitrary dimension d it is possible to find an approximate solution to the integral equation (6). This can be done by replacing the factor $(t+t')^{d-1}$ in the integrand in Eq. (6) by the factor $(2^d - 1)(t')^{d-1}$. [Such a replacement may be heuristically justified by noting that it would be exact for $\Psi(t') = \text{const}$. Also, in one dimension it becomes exact since both factors are equal to unity.] Performing this replacement, one can recast Eq. (6) into the equation

$$\frac{dN}{dt} = d\gamma\Omega_d V^d t^{d-1} \exp[-\gamma\Omega_d (Vt)^d - (2^d - 1)\, N(t)] \tag{9}$$

which can be solved exactly to give

$$N(t) = (2^d - 1)^{-1} \log[2^d - (2^d - 1)\, e^{-\gamma\Omega_d (Vt)^d}] \tag{10}$$

Combining Eqs. (7) and (10), we obtain

$$\Psi(t) = \frac{e^{-\gamma\Omega_d (Vt)^d}}{2^d - (2^d - 1)\, e^{-\gamma\Omega_d (Vt)^d}} \tag{11}$$

In one dimension, the approximate solution (10)–(11) is the exact solution of the mean-field equation (6). Numerical solutions of the nonlinear integral equation (6) for $d = 2, 3$ have revealed a good agreement between the approximate solution (10) and the numerical solution to Eq. (6), although the latter provides somewhat better agreement with Monte Carlo results.

We now develop a mean-field approximation for the touch-and-stop model with homogeneous nucleation. Let us introduce the function $\Psi(t, t_0)$ so that $\Gamma\Psi(t, t_0)\,dt_0$ gives the probability that a droplet was nucleated during the time interval (t_0, t_0+dt_0) and it is not stopped until time t, $t > t_0$. Since the number of seeds nucleating in a unit volume during the time interval $(t, t+dt)$ is $\Gamma\Phi(t)\,dt$, one has

$$\Psi(t, t) = \Phi(t) \tag{12}$$

by the definition. Consider now a droplet which has been nucleated at time t_0 at the origin and which is still growing at time t. Then in the MFT spirit we get the following estimate for $\Psi(t, t_0)$:

$$\begin{aligned}\Psi(t, t_0) = \Phi(t) \exp\left[-\beta(t-t_0)^d \left(t - \frac{t-t_0}{d+1} \right) \right] \\ \times \exp\left[-d\beta \int_0^s ds_0 \int_0^t ds\ \Psi(s, s_0)(t-t_0+s-s_0)^{d-1} \right] \\ \times \exp\left[d\beta \int_0^s ds_0 \int_0^t ds\ \Psi(s, s_0)(s-s_0)^{d-1} \right]\end{aligned} \tag{13}$$

where we have introduce the short-hand notation $\beta = \Gamma\Omega_d V^d$. The first exponential factor in Eq. (13) gives the probability that other droplets have not been nucleated in the region covered by the considered droplet. It is easily derived if one observes that it is equal to

$$\exp[-\beta(t-t_0)^d t_0] \exp\left\{ -\beta \int_{t_0}^t dt' \left[(t-t_0)^d - (t'-t_0)^d \right] \right\}$$

where the former factor is the probability that droplets did not nucleate in the ball of radius $V(t-t_0)$, centered at the origin, during the time interval $(0, t_0)$; the latter factor is the probability of the same during the time interval (t_0, t) in the untransformed part of the ball. The second exponential factor in the right-hand side of Eq. (13) estimates the probability that droplets nucleated outside of the ball have not stopped our droplet before time t. It was derived by using the expression

$$\begin{aligned}1 - d\beta\, ds_0 \int_{s_0}^t ds\ \Psi(s, s_0)(t-t_0+s-s_0)^{d-1} \\ = \exp\left[-d\beta\, ds_0 \int_{s_0}^t ds\ \Psi(s, s_0)(t-t_0+s-s_0)^{d-1} \right]\end{aligned}$$

which gives the probability that our droplet would not be stopped by a droplet nucleated during the time interval $(s_0, s_0 + ds_0)$. Multiplying all these factors for all s_0 in the interval $(0, t)$, one obtains the second exponential factor of Eq. (13). Finally, the last exponential factor of Eq. (13) and the factor $\Phi(t)$ have been introduced to guarantee that the basic relation (12) remains manifestly true.

Equation (13) should be completed by the kinetic equation

$$\frac{d\Phi}{dt} = -d\beta \int_0^t \Psi(t, t_0)(t - t_0)^{d-1}\, dt_0 \tag{14}$$

which simply follows from the fact that the radii of the droplets nucleated at time t_0 and still growing at time t are $V(t - t_0)$.

A notable feature of Eq. (13) is its simplicity in one dimension. Indeed, combining Eqs. (14) and (13), one can express the right-hand side of (13) in terms of $\Phi(t)$ only:

$$\Psi(t, t_0) = \exp[-\Gamma V(t^2 - t_0^2)]\, \Phi(t) \tag{15}$$

By inserting (15) into (14) we arrive at a closed-form equation for $\Phi(t)$:

$$\frac{d\Phi}{dt} = -2\Gamma V \Phi \int_0^t dt_0 \exp[-\Gamma V(t^2 - t_0^2)] \tag{16}$$

with solution

$$\Phi(t) = \exp\left[-2\Gamma V \int_0^t ds_1 \exp(-\Gamma V s_1^2) \int_0^{s_1} ds_2 \exp(\Gamma V s_2^2)\right] \tag{17}$$

An even more remarkable feature is that the analytical solution of the mean-field equations for the homogeneous nucleation given by Eqs. (15) and (17) turns out to be the *exact* solution. This will be confirmed in the next section, where the exact solution in one dimension will be derived rigorously.

For $d > 1$ one should solve two nonlinear equations (13)–(14) for two unknown functions $\Phi(t)$ and $\Psi(t, t_0)$ simultaneously. One can simplify these mean-field equations if, similar to the heterogeneous case, one replaces the factor $(t - t_0 + s - s_0)^{d-1} - (s - s_0)^{d-1}$ in the combined integral in Eq. (13) by the factor $B(s - s_0)^{d-1}$. We choose the constant $B = B(d)$ satisfying the condition that for constant $\Psi(s, s_0)$, after averaging on t_0 in the interval $(0, t)$, the replacement becomes exact. This yields the following value of constant B, $B = (2^{d+2} - 2)/(d + 2) - 2$. By comparison with simulational results, we have found that this replacement leads to satisfactory results. Taking into account Eq. (14) and the initial condition

$\Phi(0)=1$, we arrive at the following closed-form equation for the single variable $\Phi(t)$:

$$\frac{d\Phi}{dt}=-d\beta A\Phi\int_0^t dt_0\,(t-t_0)^{d-1}\exp\left[-\beta(t-t_0)^d\left(t-\frac{t-t_0}{d+1}\right)+B\Phi(t)\right] \tag{18}$$

with $\beta=\gamma\Omega_d V^d$ and

$$A=\exp(-B)=\exp\left(2-\frac{2^{d+2}-2}{d+2}\right)$$

Having obtained a solution to Eq. (18), one can further find $\Psi(t, t_0)$ from Eq. (14) with initial condition (12). Note also that in one dimension Eq. (18) coincides with the exact result (16).

Analyzing Eq. (18), one can find that in the long-time limit the main contribution to the integral is accumulated near the upper limit, $t_0\to t$. Computing the integral asymptotically, we find

$$t\frac{d\Phi}{dt}=-A\Phi\exp(B\Phi) \tag{19}$$

The solution to this equation decays as a power law,

$$\Phi(t)\sim t^{-A} \tag{20}$$

with the exponent $A=A(d)$ given below Eq. (18). Notice that in one dimension $A(1)=1$ and hence $\Phi(t)\sim t^{-1}$: this is the asymptotically exact result. In two dimensions our estimate of the exponent A, $A(2)=e^{-3/2}=0.223130...$, turns out to be in surprisingly good agreement with simulational result $A(2)=0.22\pm0.02$ (see Section 4).

3. EXACT SOLUTIONS IN ONE DIMENSION

It is useful to explore the kinetics of the touch-and-stop model in one dimension since exact solutions are possible to obtain in this case. We again start by considering a simpler case of the touch-and-stop process with heterogeneous nucleation. We assume that nucleation centers are distributed uniformly and independently throughout the system with density γ. Proceeding with the solution, we follow a procedure applied in refs. 19 and 20 to nucleation and growth processes. Thus we first study an auxiliary "one-sided" problem in which nuclei are scattered to the right of the origin as in the original problem but no nuclei are placed to the left of the origin.

Let $\phi(t)$ be the probability that the origin is untransformed before time t. By definition, the origin is transformed in the time interval $(t, t+dt)$ with the probability $(-d\phi/dt)\,dt$. On the other hand, it happens if the nucleus nearest to the origin lies in the space interval $(Vt, Vt+V\,dt)$ [therefore nuclei must be absent in the interval $(0, Vt)$] and the next nearest nucleus lies outside the interval $(Vt, 2Vt)$. Hence

$$\frac{d\phi}{dt}\,dt = -\gamma V\,dt \exp(-\gamma Vt)\exp(-\gamma Vt)\,\phi(t) \tag{21}$$

The last factor in Eq. (21) ensures that a second droplet does not prevent the first from reaching the origin. Integrating (22) and taking into account that initially the system is empty, $\phi(0)=1$, we obtain

$$\phi(t) = \exp\left[-\frac{1-\exp(-\gamma Vt)}{2}\right] \tag{22}$$

Let us now return to the original "two-sided" problem. Noting that the fraction of untransformed material $\Phi(t)$ is just the conditional probability for a point to be untransformed both from the left and from the right, we find the general relation between $\Phi(t)$ and $\phi(t)$:

$$\Phi(t) = \phi(t)^2 \tag{23}$$

So, the volume fraction of untransformed material is

$$\Phi(t) = \exp[\exp(-2\gamma Vt) - 1] \tag{24}$$

In particular, the limiting jammed coverage at $d=1$ is equal to $\Phi(\infty) = e^{-1} = 0.367879\ldots$. Notice that it is smaller than the jamming coverage predicted by the upper bound (3), $\Phi_{\text{upper}}(\infty)=0.5$, and larger than the jamming coverage predicted by the MFT (8), $\Phi_{\text{MFT}}(\infty) = 1-\log 2 = 0.306852\ldots$. Further, the coverage varies exponentially in the long-time limit, $\Phi(t)-\Phi(\infty) \simeq e^{-1}e^{-2\gamma Vt}$. One can observe that the true asymptotic decay is slower than that predicted by the upper bound [$\Phi(t)-\Phi(\infty) \simeq e^{-4\gamma Vt/2}$, see Eq. (3)] and similar to the one predicted by the MFT [$\Phi(t)-\Phi(\infty) \simeq e^{-2\gamma Vt/2}$, see Eq. (8)].

Let us now compute $\Psi(t)$, the probability that the growth of a droplet has not been stopped before time t. It is not difficult to establish that $\Psi(t) = e^{-2\gamma Vt}\phi(t)^2$. Here the former factor gives the probability that the interval of length $2Vt$ which is spanned by a droplet does not contain other nuclei. The latter factor ensures that both left and right ends of the droplet

at time t are untransformed by droplets nucleating from the left and right, correspondingly. Using expression (22) for $\phi(t)$, we finally obtain

$$\Psi(t) = \exp[\exp(-2\gamma Vt) - 1 - 2\gamma Vt] \tag{25}$$

From Eq. (25) one can find the density of droplets of length L in the jammed configuration, $\rho_{\text{jam}}(L)$. It follows from the general relation $\rho_{\text{jam}}(L)\, dL = \gamma(-d\Psi/dt)\, dt$ with the constraint $L = 2Vt$. Thus we find

$$\rho_{\text{jam}}(L) = \gamma^2[1 + \exp(-\gamma L)] \exp[\exp(-\gamma L) - 1 - \gamma L] \tag{26}$$

The density of droplets of length L at finite time t, $\rho(L, t)$, can be now written as

$$\rho(L, t) = \rho_{\text{jam}}(L)\, \theta(2Vt - L) + \gamma \exp[\exp(-\gamma L) - 1 - \gamma L]\, \delta(2Vt - L) \tag{27}$$

where θ is the Heaviside step function. Making use of Eqs. (26) and (27), one can calculate the fraction of untransformed material, $1 - \int_0^\infty dL\, L\rho(L, t)$, and reproduce the result given by Eq. (24), thus providing a useful check of self-consistency.

The touch-and-stop mechanism leads to the formation of clusters of stationary droplets without intervening gaps. Each cluster contains a touching pair of droplets of equal length, resulting from the first collision event in the formation of this cluster, and a number of longer droplets located to the left and to the right of the pair of shortest droplets. It seems possible to find the densities of clusters in the jammed state $\rho_{\text{jam}}(L_{-n}, \ldots, L_{-1}, L, L, L_1, \ldots, L_m)$, where $L_{-n} > \cdots > L_{-1} > L = L < L_1 < \cdots < L_m$ are the consecutive lengths of droplets in a cluster. However, we are able to compute these densities only for a few small n and m.

Consider now the touch-and-stop process with homogeneous nucleation in one dimension. It is again convenient to study first an auxiliary "one-sided" problem in which nuclei are scattered to the right and to nuclei are placed to the left of the origin. We define the probability $\phi(t)$ as in the heterogeneous problem. Thus, $(-d\phi/dt)\, dt$ is the probability that the origin is transformed during the time interval $(t, t + dt)$ by some droplet. Such a droplet could have been nucleated at any point x in the space interval $(0, Vt)$ between times $t - x/V$ and $t + dt - x/V$. Hence

$$\frac{d\phi}{dt}\, dt = -\int_0^{Vt} \Gamma\, dx\, dt \exp\left[-2\Gamma x\left(t - \frac{x}{2V}\right)\right] \phi(t) \tag{28}$$

Here $\Gamma\, dx\, dt$ is the probability of nucleation of a droplet in the space interval $(x, x + dx)$ during the time interval $(t - x/V, t + dt - x/V)$. The exponential factor and the last factor in (28) ensure that other droplets do

not prevent a droplet transforming the origin from reaching it. Actually, the exponential factor is easily derived if we observe that it is equal to

$$\exp[-2\Gamma x(t-x/V)]\exp(-2\Gamma x^2/V)$$

where the former factor is the probability that no nucleations have occurred in the interval $(0, 2x)$ during the time interval $(0, t-x/V)$, while the latter factor is the probability of the same during the time interval $(t-x/V, t)$ in the untransformed part of the space interval $(0, 2x)$. Finally, the last factor in the right-hand side of Eq. (28) ensures that droplets outside the interval $(0, 2x)$ do not stop a droplet transforming the origin before time t.

Changing variables from x to $s=t-x/V$, we recast Eq. (28) to

$$\frac{d\phi}{dt} = -\Gamma V\phi(t)\int_0^t ds\exp(\Gamma V s^2 - \Gamma V t^2) \tag{29}$$

with solution

$$\phi(t) = \exp\left[-\Gamma V\int_0^t ds_1\exp(-\Gamma V s_1^2)\int_0^{s_1} ds_2\exp(\Gamma V s_2^2)\right] \tag{30}$$

Let us now return to the original "two-sided" problem. As in the heterogeneous problem, the fraction $\Phi(t)$ of untransformed material is again related to the same function $\phi(t)$ by the constraint (23). It is now evident that the exact solution for $\Phi(t)$ completely coincides with the analytical solution (17) of the mean-field equations in one dimension. One can further simplify (17) by introducing instead of s_1 and s_2 the variables w and s_2, with $w=\Gamma V(s_1^2-s_2^2)$ and performing the integration over s_2. This yields

$$\Phi(t) = \exp\left\{-\int_0^T dw\exp(-w)\sinh^{-1}\left[\left(\frac{T}{w}-1\right)^{1/2}\right]\right\} \tag{31}$$

with $T=\Gamma V t^2$. An asymptotic analysis of Eq. (31) shows that for $T\gg 1$ the function $\Phi(t)$ decays as

$$\Phi(t) \simeq \frac{e^{-C/2}}{(4\Gamma V)^{1/2}}t^{-1} \tag{32}$$

where C is Euler's constant, $C=0.577215\ldots$.

One can obtain an exact expression for the more complex correlation function $\Psi(t, t_0)$. We do not present a derivation of this result since it turned out that the final expression coincides with the mean-field answer (15).

Using the function $\Psi(t, t_0)$, one can also find the density of droplets of length L at time t:

$$\rho(L, t) = \frac{\Gamma}{2V} \int_0^{t - L/2V} dt_2 \left[- \frac{\partial \Psi(t_1, t_2)}{\partial t_1} \right] \tag{33}$$

where t_2 is the time at which the droplet was nucleated, and t_1 is the time at which the droplet reached length L and stopped its growth, $t_1 = t_2 + L/2V$. After some algebra we finally obtain

$$\rho(L, t) = \Gamma^2 e^{\Gamma L^2/4V} \int_{L/2V}^{t} dt_1 \, \Phi(t_1) \, e^{-\Gamma L t_1} \left(t_1 + e^{-\Gamma V t_1^2} \int_0^{t_1} dt_0 \, e^{\Gamma V t_0^2} \right) \tag{34}$$

with $\Phi(t)$ given by Eq. (31).

4. NUMERICAL SIMULATIONS

Numerical simulations of the growth kinetics were performed for both heterogeneous and homogeneous nucleation models. In the case of homogeneous model, we also investigated the fractal properties of emerging patterns.

To simulate the heterogeneous model in two and three dimensions, about 10^3 nucleation sites were distributed randomly and simulations were

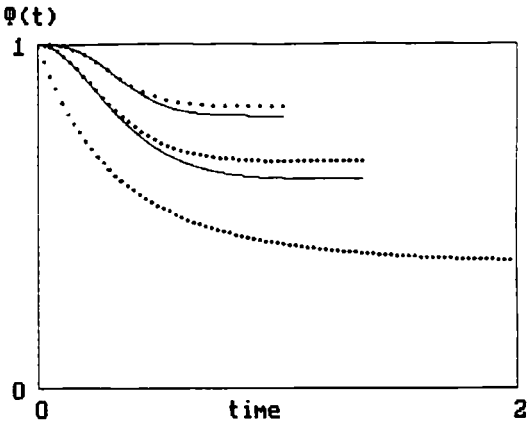

Fig. 1. The fraction of untransformed material $\Phi(t)$ versus the dimensionless time t for the heterogeneous nucleation model. We present results for one-dimensional (the lower curve) two-dimensional (the middle pair of curves), and three-dimensional (the upper pair) systems. Mean-field result are shown by solid lines. Results of Monte Carlo simulations for $d = 2$ and 3 and the exact solution for $d = 1$ are shown by dots. The unit of time for the d-dimensional heterogeneous nucleation model is equal to $\gamma^{-1/d} V^{-1}$.

repeated 100–150 times. For the homogeneous nucleation model, nucleation sites have been generated with a constant rate and simulations proceeded until the overall number of nucleation sites reached 240,000. In all simulations we used the periodic boundary conditions.

We evaluated the fraction of untransformed area $\Phi(t)$ and compared it with the mean-field predictions. For the heterogeneous nucleation model, numerical and mean-field results for 2D and 3D systems and exact results in one dimension are presented in Fig. 1. One can see that mean-field predictions differ quantitatively from exact and numerical results for all $d = 1$–3. For example, the jammed fraction of untransformed material $\Phi(\infty)$ is equal to $e^{-1} = 0.367879...$, 0.660 ± 0.005, and 0.82 ± 0.01 for $d = 1$, 2, and 3, respectively. On the other hand, the MFT predicts 0.306852..., 0.612..., and 0.79..., respectively. Notice that the heterogeneous nucleation model leads to less dense jammed coverage than the (continuum) RSA of disks, which gives the jammed fraction of uncovered material equal to 0.252402... ($d = 1$) and 0.4528 ± 0.0002 ($d = 2$). However, the kinetic behavior that emerges from the MFT and even from the simplified MFT (10)–(11) turns out to be in a good qualitative agreement with numerical results.

Results for the homogeneous nucleation model are presented in Fig. 2. Simulations show that for the 2D system the fraction of untransformed area $\Phi(t)$ decays as a power law in the long-time limit. When the dimensionless time t [the time in the 2D homogeneous nucleation model is measured in units of $(\Gamma V^2)^{-1/3}$] varies from 100 up to the maximum

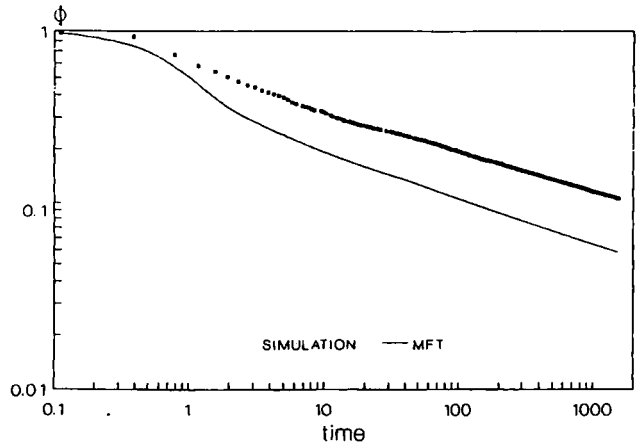

Fig. 2. The fraction of untransformed material $\Phi(t)$ versus the dimensionless time t for the 2D homogeneous nucleation model. The unit of time for the 2D homogeneous nucleation is equal to $\Gamma^{-1/3}V^{-2/3}$.

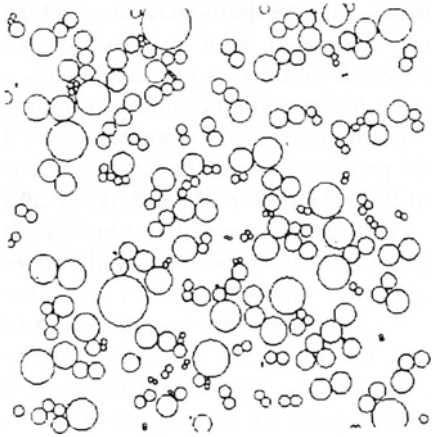

Fig. 3. The final pattern for the 2D heterogeneous nucleation model.

simulation time 1600, we found that $\Phi(t) \sim t^{-A}$, with $A = 0.22 \pm 0.01$. Notice that the simplified version of the MFT, Eq. (18), predicts in the 2D case a very close value of A, $A = e^{-3/2} = 0.223130...$ [see Eq. (20)].

The geometrical properties of emerging patterns are very different for the heterogeneous and homogeneous nucleation models. In Fig. 3, the typical final pattern for the 2D heterogeneous nucleation model is shown. One can observe that the pattern is formed by separated "tree"-type clusters of 2–10 particles. In Fig. 4 we plot the pattern for the 2D homogeneous

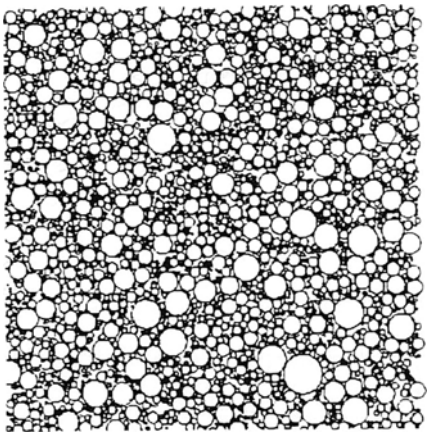

Fig. 4. The pattern for the 2D homogeneous nucleation model at the dimensionless time $t = 70$.

nucleation model at time $t = 70$. Notice that the pattern looks like a self-similar fractal object. To study the fractal properties of arising 2D patterns we used the following procedure.[21] We computed an average number of nucleating sites $\langle n(l) \rangle$ in a box of size $l * l$. The centers of boxes were placed at some randomly chosen nucleation sites. Computations were performed for the pattern consisting of 240,000 particles, obtained at (dimensionless) time $t = 1600$. For each l, approximately 10^3 boxes were used.

In Fig. 5 we plot the dependence of $\ln[\langle n(l) \rangle]$ versus $\ln(l)$. One can see that at $l \simeq 0.6$ [the length in the 2D homogeneous nucleation model is measured in units of $(V/\Gamma)^{1/3}$] a crossover from the dependence $\langle n(l) \rangle \sim l^2$ to the dependence $\langle n(l) \rangle \sim l^{D_f}$, with $D_f \simeq 1.75$, takes place. The former dependence characterizes the two-dimensional patterns, while the latter indicates the fractal structure of the pattern at sufficiently small sizes. The present procedure gives the same numerical value of fractal dimension $D_f \simeq 1.75$ for all patterns arising at $t > 300$, thus emphasizing that the homogeneous nucleation model really evolves toward the fractal pattern. Such a conclusion is further supported by the fact that the homogeneous version of our touch-and-stop model is the generalized version of the random space-filling-bearing model.[15] Structures arising in the latter model are surely fractals.[15] For a nonrandom space-filling-bearing model, e.g., for the Apollonian packing, which is probably the first example of a fractal in science (it was introduced 200 BC by Apollonius of Perga), the fact that the patterns are fractals was proved rigorously[22] and confirmed by precise numerical simulations.[23]

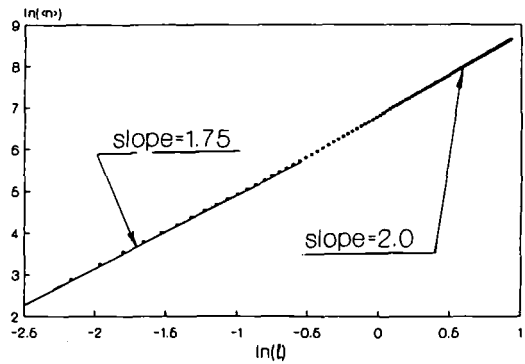

Fig. 5. Plot of $\ln[\langle n(l) \rangle]$ versus $\ln(l)$ at dimensionless time $t = 1600$ in the case of 2D homogeneous nucleation. The time and length are measured in the units $(\Gamma V^2)^{-1/3}$ and $(V/\Gamma)^{1/3}$, respectively. The small-scale slope 1.75 indicates the fractal structure of the pattern.

5. CONCLUSIONS

We have introduced a novel touch-and-stop model of growth in which droplets grow from nucleation sites and stop growing when two or more droplets touch. We have investigated two extreme cases of homogeneous and heterogeneous nucleation. The present model combines the properties of both nucleation-and-growth and RSA models. The homogeneous variant of our model in the limiting case of infinitely rapid growth turns into the random Apollonian packing.

The growth kinetics as well as geometrical properties of emerging patterns have been examined. We have written the mean-field equations and solved them exactly in one dimension for both heterogeneous and homogeneous nucleation. For $d>1$ we found approximate solutions of the mean-field equations in the case of heterogeneous nucleation. We found that the fraction of untransformed material $\Phi(t)$ approaches the jammed state as $\Phi(t)-\Phi(\infty)\sim\exp[-\gamma\Omega_d(Vt)^d]$ and estimated the jammed fraction of uncovered volume $\Phi_{\mathrm{MFT}}(\infty)=1-d\log(2)/(2^d-1)$. For the case of homogeneous nucleation we estimated the long-time decay of the fraction of untransformed material. We obtained exact solutions in one dimension for both heterogeneous and homogeneous cases. For two- and three-dimensional systems numerical simulations have been carried out. Mean-field predictions turn out to be in a good qualitative agreement with exact and numerical results.

For the touch-and-stop model with heterogeneous nucleation we found that in arbitrary dimension the system reaches the jamming limit in which the fraction of untransformed material is equal to $e^{-1}=0.367879...$ ($d=1$), 0.660 ± 0.005 ($d=2$), 0.82 ± 0.01 ($d=3$). For the touch-and-stop model with homogeneous nucleation we have found numerically that the fractal dimension for the space-filling pattern is $D_f\simeq 1.75$.

ACKNOWLEDGMENTS

N.V.B. is supported by Max-Planck-Gesellschaft. P.L.K. is supported by ARO grant DAAH04-93-G-0021 and NSF grant DMR-9219845.

REFERENCES

1. J. W. Cristian, *The Theory of Phase Transformations in Metals and Alloys, Part I: Equilibrium and General Kinetic Theory* (Pergamon Press, New York, 1981).
2. J. D. Gunton and M. Droz, *Introduction to the Theory of Metastable and Unstable States* (Springer-Verlag, New York, 1983).
3. R. J. Field and M. Burger, eds., *Oscillations and Travelling Waves in Chemical Systems* (Wiley, New York, 1985).

4. D. Beysens and C. M. Cnobler, *Phys. Rev. Lett.* **57**:1433 (1986).
5. J. A. Glazier and D. Weaire, *J. Phys. Cond. Matter* **4**:1867 (1992).
6. A. T. Florence, T. K. Law, and T. L. Whatley, *J. Colloid Interface Sci.* **107**:584 (1985).
7. B. J. Mason, *The Physics of Clouds* (Oxford University Press, Oxford, 1957).
8. R. Zallen, *The Physics of Amorphous Solids* (Wiley, New York, 1983).
9. K. J. Maloy, J. Feder, and T. Jossang, *Phys. Rev. Lett.* **55**:2688 (1985).
10. B. Lewis and J. C. Anderson, *Nucleation and Growth of Thin Films* (Academic Press, New York, 1978).
11. M. Hasegawa and M. Tanemura, *Ann. Inst. Stat. Math. B* **28**:509 (1976).
12. J. W. Evans, *Rev. Mod. Phys.* **65**:1281 (1993).
13. K. Sekimoto, *Int. J. Mod. Phys. B* **5**:1843 (1991).
14. H. J. Herrmann, G. Mantica, and D. Bessis, *Phys. Rev. Lett.* **65**:3223 (1990); H. J. Herrmann, *Pour la Sci.* **165**:17 (1991).
15. S. S. Manna, *Physica A* **187**:373 (1992).
16. B. B. Mandelbrot, *The Fractal Geometry of Nature* (Freeman, San Francisco, 1982).
17. S. Chandrasekhar, *Rev. Mod. Phys.* **15**:1 (1943).
18. I. M. Lifshitz, *Adv. Phys.* **13**:483 (1964).
19. R. M. Bradley and P. N. Strenski, *Phys. Rev. B* **40**:8967 (1989).
20. Yu. A. Andrienko, N. V. Brilliantov, and P. L. Krapivsky, *Phys. Rev. A* **45**:2263 (1992); P. L. Krapivsky, *J. Chem. Phys.* **97**:8817 (1992).
21. T. Vicsek, *Physica A* **168**:490 (1990).
22. D. W. Boyd, *Mathematica* **20**:170 (1973).
23. S. S. Manna and H. J. Herrmann, *J. Phys. A* **24**:L481 (1991).